An Accurate Virtual Signal Injection Control of MTPA for an IPMSM With Fast Dynamic Response

Jun Wang, *Student Member, IEEE*, Xiaoyan Huang, *Member, IEEE*, Dong Yu, Yuzheng Chen, Jian Zhang, Feng Niu, *Member, IEEE*, Youtong Fang, *Member, IEEE*, Wenping Cao, *Senior Member, IEEE*, and He Zhang, *Member, IEEE*

***Abstract*—A maximum torque per ampere (MTPA) control based on virtual signal injection for an interior permanent magnet synchronous motor with fast dynamic response is proposed in this paper. A small square wave signal is mathematically injected into the current angle for accurately tracking MTPA points. The extracted derivative of electromagnetic torque is utilized to compensate the initially set current angle to the real MTPA operation current angle. Due to the absence of bandpass and low-pass filters, which are essential in the sinusoidal injected signal scheme, this method shows good dynamic response. By incorporating a modified equation for the torque after signal injection, the steady-state accuracy is also enhanced. The d- and q-axis current references are obtained through the current vector magnitude and optimal current angle instead of using the torque equation with nominal motor parameters, which guarantees the accuracy of the output torque. The proposed scheme is parameter independent, and no real signal is injected to the current or voltage command. Thus, the problems of the high-frequency signal injection method are avoided. A prototype is set up, and experiments are carried out to verify effectiveness and robustness of the proposed control scheme.**

***Index Terms*—Interior permanent magnet synchronous motor (IPMSM), maximum torque per ampere (MTPA), virtual signal injection.**

I. Introduction

THE interior permanent magnet synchronous motors (IPMSMs) are widely used in various applications due to their merits such as high power/torque density, high efficiency, high power factor and robustness over other ac motors, and excellent field-weakening performance [1], [2]. To fully utilize the reluctance torque of the IPMSM, maximum torque per ampere (MTPA) operation is preferred, and it can be realized by controlling the current angle using the motor parameters under a certain stator current [3]. However, the parameters of the IPMSM exhibit obvious nonlinear characteristics due to magnetic saturation, cross-coupling effect, and temperature dependence. Thus, the perfect MTPA point tracking in practical applications is usually difficult.

The MTPA points are usually calculated using constant nominal parameters [3], [4]. However, the d- and q-axis inductances and permanent flux linkage may decrease dramatically due to the magnetic saturation, which severely deteriorates the accuracy of MTPA point tracking [5], [6]. Various methods have been presented to deal with this problem, and they can be classified into two categories: the offline ones and online ones.

For the offline procedures, the d- and q-axis current references for MTPA points considering parameter variations are usually obtained from the lookup table (LUT), which is generated based on offline experiments or finite-element method (FEM) simulations [7]–[9]. For an accurate control, both of magnetic saturation and demagnetization should be considered, and hence, massive experiments or simulations have to be carried out, which is time-consuming. In [10], a simpler LUT is set up at the cost of a relatively complicated control scheme. The d- and q-axis current references are updated based on the LUT each iteration until they converge to certain values. However, such an iteration algorithm may lead to a convergence problem.

For the online methods, it can be basically divided into two categories: the online parameter estimation and virtual signal injection. To deal with the parameter variation problem, one typical solution is estimating the real-time parameters, and different estimation algorithms have been proposed, such as recursive least squares [11], [12] and affine projection algorithm [13], [14]. In [13], only q-axis inductance and permanent flux linkage are estimated to avoid the rank-deficient problem, and the estimation algorithm is combined with a self-correction scheme to realize the real-time MTPA tracking. However, the variation of d-axis inductance and resistance may deteriorate the tracking accuracy. In [11], [12], and [14], additional signals are injected to estimate all four parameters, but additional copper loss is inevitable. A backstepping control scheme based on the Lyapunov criterion was first proposed in [15] to realize the zero d-axis

Manuscript received June 12, 2017; revised September 1, 2017; accepted October 12, 2017. Date of publication October 18, 2017; date of current version June 22, 2018. This work was supported in part by the National Natural Science Foundation of China under Grant 51477149 and Grant U143420005, in part by the National Sci-Tech Support Plan under Grant 2015BAG13B01-08 and in part by the Natural Science Foundation of Zhejiang Province under Grant LY16E070001. Recommended for publication by Associate Editor L. Dalessandro. *(Corresponding author: Jian Zhang.)*

J. Wang, X. Huang, D. Yu, Y. Chen, J. Zhang, and Y. Fang are with the College of Electrical Engineering, Zhejiang University, Hangzhou 310027, China (e-mail: 3100100810@zju.edu.cn; xiaoyanhuang@zju.edu.cn; kevinyu_zju@163.com; chenyuzheng@zju.edu.cn; jian_zhang_zju@zju.edu.cn; youtong@zju.edu.cn).

F. Niu is with the College of Electrical Engineering, Zhejiang University, Hangzhou 310027, China, and also with the State Key Laboratory of Reliability and Intelligence of Electrical Equipment, Hebei University of Technology, Tianjin 300130, China (e-mail: niu.feng.hebut@gmail.com).

W. Cao is with the School of Engineering and Applied Science, Aston University, Birmingham B4 7ET, U.K. (e-mail: w.p.cao@aston.ac.uk).

H. Zhang is with the University of Nottingham Ningbo China, Ningbo 315100, China (e-mail: he.zhang@nottingham.edu.cn).

Color versions of one or more of the figures in this paper are available online at http://ieeexplore.ieee.org.

Digital Object Identifier 10.1109/TPEL.2017.2764500

current control, and the scheme is extended to MTPA control in [16]. This control scheme replaces the traditional proportional–integral (PI) controller by a backstepping controller with the parameters updated in each control period. However, the computation burden is heavy, which may result in stability issues. In recent years, some signal injection methods have been proposed to track the real-time MTPA points [17]–[19]. These control schemes are parameter independent, and the accuracy of the MTPA tracking is satisfactory. However, as mentioned before, the additional injected signal brings additional copper loss as well.

A virtual signal injection method to track the MTPA operation points is proposed in [20]. A small sinusoidal signal is injected to the current angle, and the torque derivative is obtained through various filters to generate the desired d-axis current. This control scheme can track the MTPA operation points, but the dynamic response is quite slow due to the use of overmuch filters, and the steady-state error is unbearable. To improve the dynamic control performance, a self-learning controller based on virtual signal injection is proposed in [21]. The controller is trained online and operates well if the same operation condition has been trained before. However, the dynamic performance is still unsatisfactory when the operation conditions are first encountered, and in practical applications, the operation condition, i.e., the torque command, may vary in a such a large range that it is time-consumed to train every operation condition.

In this paper, a novel virtual signal injection method with fast dynamic response and accurate MTPA point tracking is proposed. A square injection signal removes the utilization of cascaded filters, which leads to a fast dynamic response. The method to obtain command stator current amplitude is discussed in detail for torque control. No real signal is injected to the motor, and hence, the problems associated with high-frequency signal injection methods are avoided. Based on the analysis of the characteristic of the virtual signal injection method, the modified equation of electromagnetic torque considering signal injection is proposed to enhance the MTPA tracking accuracy. A simple compensation method is utilized to generate the current vector magnitude reference. The simulations and experiments are conducted on MATLAB/Simulink and a prototype IPMSM drive system with dSPACE to support the claims.

II. System Model With an Injected Signal

The mathematical model of an IPMSM in a synchronously rotating dq frame can be expressed as

$$\begin{aligned} v_d &= R_s i_d + pL_d i_d + e_d \\ v_q &= R_s i_q + pL_q i_q + e_q \\ e_d &= -\omega_e L_q i_q \\ e_q &= \omega_e (L_d i_d + \psi_f) \\ T_e &= \frac{3}{2}\frac{P}{2}[\psi_f i_q + (L_d - L_q) i_d i_q] \end{aligned} \tag{1}$$

where v_d and v_q are the synthesized voltages in the dq frame applying to the motor terminal from a pulse width modulation inverter; i_d and i_q are the currents in the dq frame; R_s, L_d, and L_q represent the stator resistance, the d-axis stator inductance, and the q-axis stator inductance, respectively; e_d and e_q denote the effective back EMFs of d- and q-axes, respectively; ω_e and ψ_f are electrical angular velocity and stator flux linkage of the permanent magnet; p is the differential symbol; and P represents the number of poles.

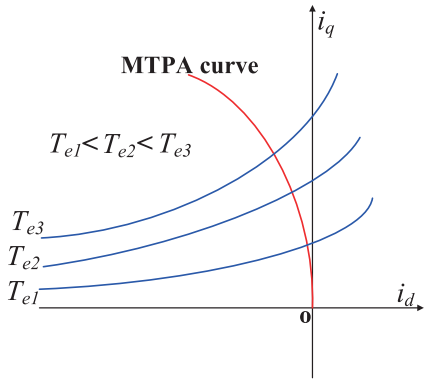

Fig. 1. MTPA and constant torque curves.

The electromagnetic torque consists of two parts, i.e., the interaction of permanent magnet flux linkage with q-axis current and the reluctance torque due to the rotor saliency. For a given magnitude of the current vector, the torque equation can be rewritten as a function of current angle as follows:

$$T_e(\beta) = \frac{3}{2}\frac{P}{2}\left[\psi_f I_s \cos\beta - \frac{1}{2}(L_d - L_q) I_s^2 \sin 2\beta\right] \tag{2}$$

where I_s is the magnitude of current vector and β is the current angle between current vector and q-axis. The MTPA operation points are the points on the constant torque curves that have the minimum stator current magnitude. As can been seen in Fig. 1, the MTPA locus is vertical to the constant torque curve, and the optimal current angle β for MTPA control can be derived by setting $\partial T_e/\partial\beta$ to zero [22] as

$$\beta = \sin^{-1}\frac{-\psi_f + \sqrt{\psi_f^2 + 8(L_q - L_d)^2 I_s^2}}{4(L_q - L_d) I_s}. \tag{3}$$

Theoretically speaking, if the current angle is kept consistent with the result of (3) during the operation, the motor can track the MTPA operation points. However, L_d and L_q vary from the nominal values due to the magnetic saturation and ψ_f may decrease greatly as the temperature gets higher. Hence, the optimal current angle deviates seriously from the calculated one of (3) using nominal values of motor parameters, which leads to the poor MTPA tracking.

The relationship between the current angle and torque with a fixed current vector magnitude is illustrated in Fig. 2. It is evident that $\partial T_e/\partial\beta$ is positive when the current angle is smaller than the optimal one and is negative when the current angle is greater than the optimal one. According to this feature, a small signal can be injected into the current angle to obtain the value of $\partial T_e/\partial\beta$, and then, the MTPA operation points can be accurately tracked according to the value of $\partial T_e/\partial\beta$.

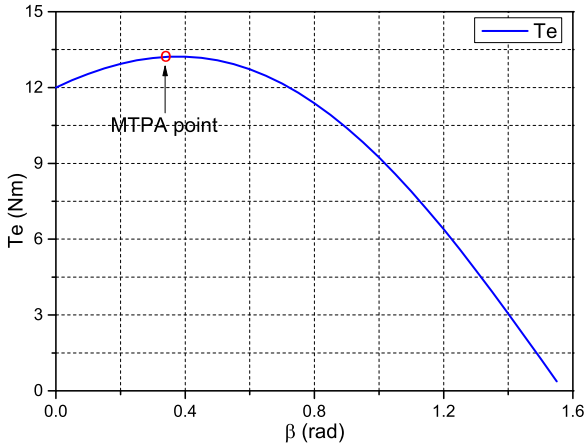

Fig. 2. Relationship between the current angle and the torque under a fixed current vector magnitude.

In this work, a 50% duty cycle square wave expressed by (4) is utilized as the injection angle variation, where T_s represents the signal period, A is the amplitude of the injection signal, and N denotes the nature number set:

$$\gamma(t) = \begin{cases} 0, & NT_s \leqslant t < (N+\frac{1}{2})T_s \\ A, & (N+\frac{1}{2})T_s \leqslant t < (N+1)T_s. \end{cases} \tag{4}$$

Combining (2) and (4) gives

$$T_e^h(\gamma) = \frac{3}{2}\frac{P}{2}\left[\psi_f I_s \cos(\beta+\gamma) - \frac{1}{2}(L_d - L_q) I_s^2 \sin 2(\beta+\gamma)\right] \tag{5}$$

where T_e^h represents the electromagnetic torque after signal injection.

III. Proposed Virtual Signal Injection Method

A. Current Angle Compensation

Assuming that (5) is a function of γ and using Taylor's series expansion around the origin yields

$$\begin{aligned} T_e^h(\gamma) &= T_e^h(0) + \frac{\partial T_e^h}{\partial \gamma}|_{\gamma=0}\gamma + \frac{1}{2}\frac{\partial^2 T_e^h}{\partial^2 \gamma}|_{\gamma=0}\gamma^2 + \cdots \\ &= T_e(\beta) + \frac{\partial T_e}{\partial \beta}\gamma + \frac{1}{2}\frac{\partial^2 T_e}{\partial^2 \beta}\gamma^2 + \cdots. \end{aligned} \tag{6}$$

Because the amplitude of the injection signal A is quite small, the first-order term in (6) is dominant in torque variation compared with the other high-order components. Thus, Taylor's series can be truncated after the first-order term:

$$T_e^h(\gamma) = T_e(\beta) + \frac{\partial T_e}{\partial \beta}\gamma. \tag{7}$$

In (7), $T_e(\beta)$ indicates the torque without injection signal, i.e., the electromagnetic torque of the motor. It can be calculated using (1). But, as mentioned before, the motor parameters may deviate from its nominal values greatly, so the torque can be calculated using the mechanical power. The mechanical power without iron loss considered can be expressed as

$$P_m = \frac{3}{2}[(v_d - Ri_d)i_d + (v_q - Ri_q)i_q]. \tag{8}$$

As an alternative, $T_e(\beta)$ can be obtained from

$$\begin{aligned} T_e(\beta) = \frac{P_m}{\omega_m} &= \frac{3}{2\omega_m}[(v_d - Ri_d)i_d + (v_q - Ri_q)i_q] \\ &= \frac{3}{2\omega_m}[-(v_d + RI_s\sin\beta)I_s\sin\beta \\ &\quad + (v_q - RI_s\cos\beta)I_s\cos\beta] \end{aligned} \tag{9}$$

where ω_m represents the mechanical angular velocity and satisfies the relationship $\omega_e = \frac{P}{2}\omega_m$.

In [20], the electromagnetic torque after signal injection is calculated by

$$T_e^h = \frac{3}{2}\left[\frac{v_q - Ri_q}{\omega_m} + \frac{v_d - Ri_d}{i_q\omega_m}i_d^h\right]i_q^h \tag{10}$$

where i_d^h and i_q^h represent the d- and q-axis current after signal injection, respectively. However, the accuracy of results obtained from this equation is intolerable.

The electromagnetic torque after signal injection can be accurately calculated by

$$\begin{aligned} T_e^h &= \frac{3}{2}\frac{P}{2}\left[\psi_f i_q^h + (L_d - L_q)i_d^h i_q^h\right] \\ &= \frac{3}{2}\frac{P}{2}\left[\psi_f i_q^h + L_d i_d^h i_q^h - L_q i_d^h i_q^h\right]. \end{aligned} \tag{11}$$

However, the accuracy of (11) depends heavily on the accurate knowledge of motor parameters, which deviates from their nominal values during the operation. Thus, (10) should be modified to approach the value obtained by (11).

In steady-state operation, the voltage equation can be rewritten as

$$v_d - Ri_d = -\omega_e L_q i_q \tag{12}$$

$$v_q - Ri_q = \omega_e\psi_f + \omega_e L_d i_d. \tag{13}$$

The third term in the bracket of (11) can be easily obtained through (12)

$$\frac{v_d - Ri_d}{\omega_e i_q}i_d^h i_q^h = -L_q i_d^h i_q^h. \tag{14}$$

From (13), the first two terms in the bracket of (11) can be calculated by

$$\begin{aligned} \psi_f i_q^h + L_d i_d^h i_q^h &= (\psi_f + L_d i_d)i_q^h + L_d i_q^h(i_d^h - i_d) \\ &= \frac{v_q - Ri_q}{\omega_e}i_q^h + L_d i_q^h(i_d^h - i_d). \end{aligned} \tag{15}$$

As the amplitude of the injected signal γ is very small, i_d^h can be expressed as

$$i_d^h = -I_s\sin(\beta+\gamma) \approx -I_s\sin\beta - \gamma I_s\cos\beta = i_d - i_q\gamma. \tag{16}$$

Substituting (16) into (15) yields

$$\psi_f i_q^h + L_d i_d^h i_q^h = \left(\frac{v_q - Ri_q}{\omega_e} - L_d i_q\gamma\right)i_q^h. \tag{17}$$

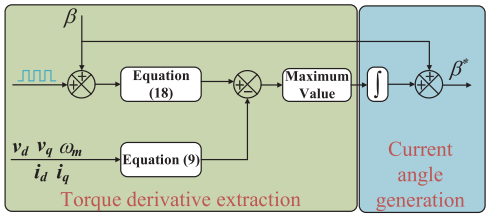

Fig. 3. Schematic of the signal-processing technique.

Hence, T_e^h can be expressed as

$$T_e^h(\gamma) = \frac{3}{2\omega_m}\left[\frac{v_d - Ri_d}{i_q} i_d^h i_q^h + (v_q - Ri_q - \omega_e L_d i_q \gamma)\, i_q^h\right]. \tag{18}$$

The d-axis inductance may deviate from its nominal value due to magnetic saturation. However, compared to q-axis inductance, the variation of d-axis inductance is smaller because the flux in the d-axis is intense and the d-axis is somewhat saturated under the no-load condition. In addition, the small amplitude of γ also reduces the impacts of varied d-axis inductance.

The value of $\gamma \partial T_e / \partial \beta$ can be obtained by combining (4), (7), (9), and (18) as

$$\frac{\partial T_e}{\partial \beta}\gamma(t) = \begin{cases} 0, & NT_s \leqslant t < (N+\frac{1}{2})T_s \\ \frac{\partial T_e}{\partial \beta} A, & (N+\frac{1}{2})T_s \leqslant t < (N+1)T_s. \end{cases} \tag{19}$$

The maximum value of (19) is extracted and updated in each control cycle. Utilizing a pure integral, the current angle compensation value is added to an initial current angle to track the optimal current angle. The schematic diagram of the signal processing technique is illustrated in Fig. 3.

B. Current Vector Magnitude Generation

The current vector magnitude is also a key factor as it determines the maximum output torque. In some applications, the purpose of control system is to generate the desired torque rather than keeping the speed constant, and hence, the input command of motor control system is the torque reference. The ideal relationship between torque and current vector magnitude for a permanent magnet motor is linear

$$T_e = K_t I_s \tag{20}$$

where K_t is the constant torque coefficient under the ideal condition. However, the motor parameters may vary according to the operating condition, so that the torque coefficient cannot remain constant in practical applications. Thus, a classical open-loop approach in parallel to the closed-loop approach based on an integral controller is utilized to compensate the current vector magnitude shown as follows:

$$I_s = \frac{T_e^*}{K_t} + \frac{K_{ti}(T_e^* - T_e)}{s} \tag{21}$$

where T_e^* and T_e are the torque reference and output torque calculated by (9), respectively, and K_{ti} represents the integrator coefficient. The scheme of current vector magnitude generation in the torque mode is given in Fig. 4.

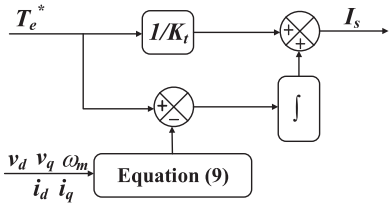

Fig. 4. Current vector magnitude generation in the torque mode.

C. Control System

The optimal angle and magnitude of the current vector can be obtained through the aforementioned method, and the d- and q-axis current references can be expressed as

$$\begin{aligned} i_d^* &= -I_s \sin\beta^* \\ i_q^* &= I_s \cos\beta^*. \end{aligned} \tag{22}$$

Thus, the current references in (22) can accurately represent the actual MTPA points and PI controller is utilized to force the real currents to track the references. The control system is illustrated in Fig. 5. The detailed schematic of the current angle and vector magnitude generator are the ones illustrated in Figs. 3 and 4.

IV. Simulation Results

Simulation based on MATLAB/Simulink is carried out to validate the effectiveness of the proposed virtual signal injection control. Nominal parameters of the IPMSM are given in Table I. The inverter switching frequency is 5 kHz, and the frequency of injection square wave is 1 kHz, i.e., the signal period T_s is 1 ms. The PI current controller is designed with the zero-pole-elimination principle, and the bandwidth is set to 200 Hz.

The inductances and permanent magnet flux linkage of the IPMSM under different load conditions are obtained using the FEM, as illustrated in Fig. 6. Obviously, the variation of inductance in the q-axis is severe than that of the d-axis, and due to the variation of d-axis inductance, q-axis inductance, and permanent magnet flux linkage, the MTPA points may deviate from the points obtained with nominal values.

To demonstrate the fast dynamic response of the proposed method, the IPMSM simulations in the torque mode with the speed held at 300 r/min during the whole operation are carried out, and the sinusoidal signal injection method in [20] is taken as a comparison. The torque command changes abruptly from 5 to 10 N·m at 1.0 s, and the d- and q-axis currents are illustrated in Fig. 7.

As mentioned before, the cascaded filters in [20] severely deteriorate the dynamic performance and it takes 0.7 s for the motor to come into the steady mode. The proposed method, however, shows a better dynamic performance with only 0.05 s transient process. It is also obvious that the two methods converge to different operation points. This difference comes from the different calculation methods of T_e^h, and the accuracy of the two methods is given in Fig. 8.

In Fig. 8, the blue curve is the MTPA operating line obtained using the FEM results in Fig. 6. As can been seen, the sinusoidal

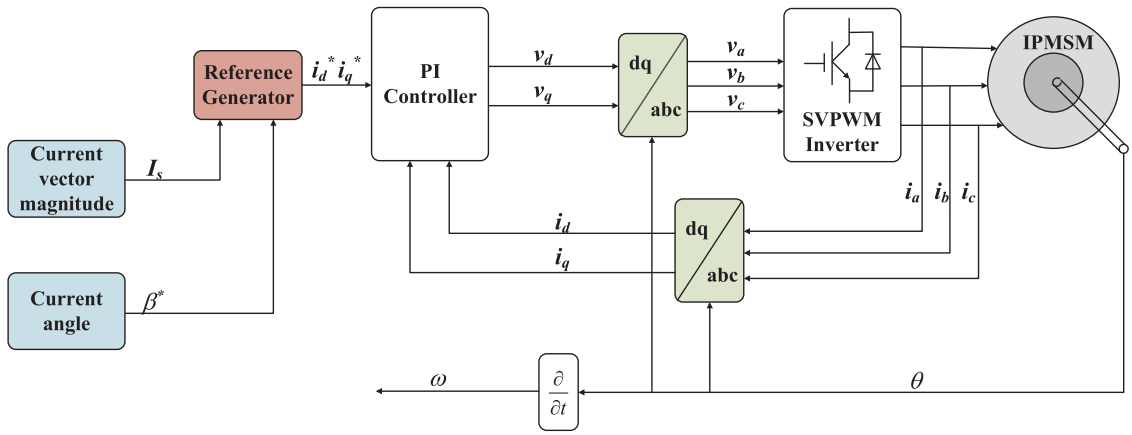

Fig. 5. Control system diagram.

TABLE I
PARAMETERS OF THE TESTED IPMSM

P	4
R_s	4.31 Ω
ψ_f	0.936 Wb
L_d	56 mH
L_q	119 mH
$V_{\rm DC}$	300 V
$I_{s,\max}$	8 A
$P_{\rm rated}$	2 kW
$n_{\rm rated}$	800 r/min

signal injection method deviates a lot from the MTPA line due to the inappropriate calculation of T_e^h, and the points obtained by (18) reveal better accuracy.

Another simulation is carried out to verify the robustness of the proposed method. The motor is running in the torque mode at the speed of 800 r/min, and the torque command increases or decreases 2 N·m every 0.2 s.

The output torque and the current angle are illustrated in Fig. 9, and the d- and q-axis currents are given in Fig. 10. As clearly shown, the proposed method is robust with fast transient response.

V. EXPERIMENTAL RESULTS

A test bench shown in Fig. 11 is set up to verify the proposed method, and the motor parameters are the same as that given in Table I. The IPMSM is controlled in the torque mode at a certain speed driven by the asynchronous motor, and the motor torque is measured by a torque transducer JN338-A-50. The controller's sampling rate is 5 kHz and the carrier frequency is also 5 kHz. The frequency of the injection signal has to be lower than the control frequency, and it is selected as 1 kHz. The amplitude of the injected signal is 0.002 V.

The first set of tests is performed with the torque command varying from 1 to 20 N· m in a step of 1 N· m every 2 s at the speed of 300 r/min. To demonstrate the accuracy of the proposed method, the sinusoidal signal injection method proposed in [20] is still carried out as a comparison. Using the FEM results of L_d, L_q, and ψ_f, the MTPA curve is obtained by the Newton–Raphson iteration method, and the results are given in Fig. 12.

As can been clearly seen, the proposed method possesses a better MTPA tracking accuracy compared with the sinusoidal signal injection method, which uses (10). The tracking MTPA points of the proposed method do not exactly lie on the MTPA curve mainly due to the dead zone effect of the inverter and the variation of d-axis inductance. The current vector magnitudes of the proposed method and the sinusoidal signal injection method are listed in Table II. The higher the torque reference, the larger the current vector magnitude difference.

To further demonstrate the accuracy of the proposed method, Fig. 13 illustrates the current waveform of phase A of the proposed method and the sinusoidal signal injection method at the speed of 300 r/min with 35-N·m torque command. The root-mean-square value of I_a for the two methods are 8.24 and 8.51 A, respectively. In other words, least current is needed under the same torque for the proposed method, and hence, a better MTPA tracking accuracy is achieved. As the torque gets higher, the current differences among the two methods will be larger.

The waveforms of dq-axis currents and the output torque and the current angle are shown in Fig. 14(a) and (b), respectively. The extracted value of $\partial T_e/\partial\beta$ is utilized to generate the current angle rather than d-axis current reference through an integrator. Normally, the current angle varies in a smaller range than that of d-axis current reference, and the square wave injection signal removes the cascaded filter. Hence, the dynamic response of the proposed method is better. Although the current angle may not converge to the steady value as fast as other variables, it quickly approaches the steady value and the variations of the dq-axis current references are pretty small afterwards. The overshoots of the output torque at each step are caused by the inappropriate torque coefficient and invalidity of (9) during fast transient, but with the help of current vector magnitude generation using (21), the output torque quickly converges back to the torque command.

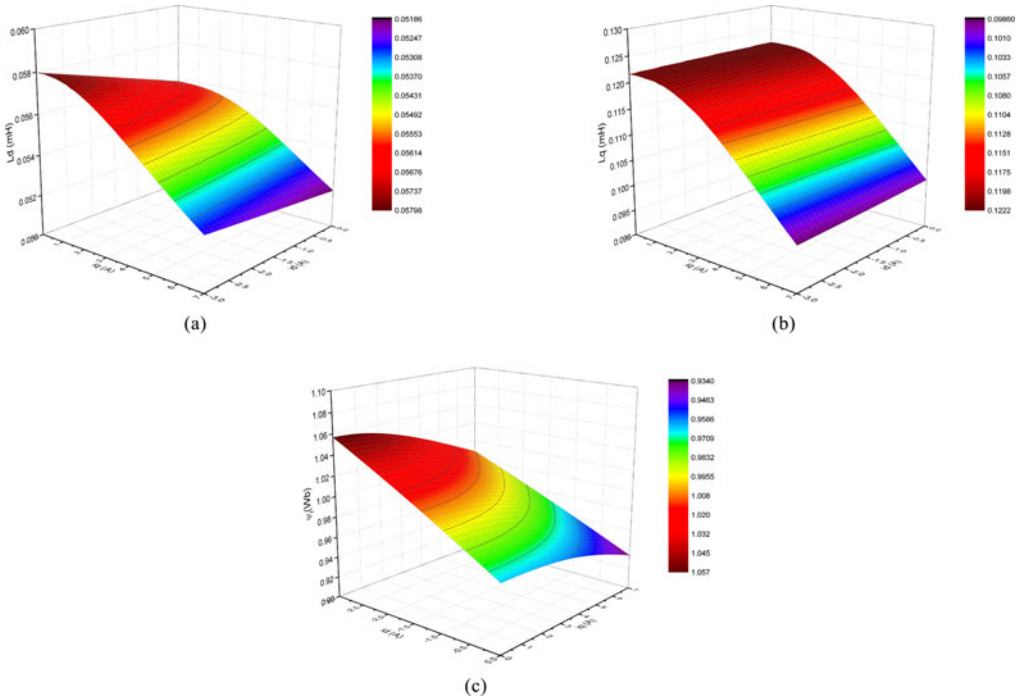

Fig. 6. Nonlinear IPMSM motor parameters. (a) d-axis inductance as a function of dq-axis currents. (b) q-axis inductance as a function of dq-axis currents. (c) Permanent magnet flux linkage as a function of dq-axis currents.

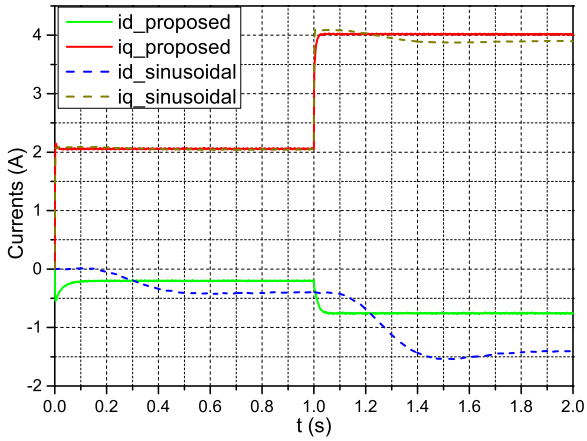

Fig. 7. Dynamic performances of the proposed method and the sinusoidal injection.

To prove the accurate output torque and fast dynamic response of the proposed scheme, the equation for T_e^h in the sinusoidal injection method is changed to (18) as well. The IPMSM is held at 300 r/min with a step increase of torque reference from 11 to 22 N·m. The experimental results are illustrated in Fig. 15.

As can be seen in Fig. 15(a), the proposed method possesses obvious better dynamic response. The sinusoidal injection method utilizes torque derivative to generate d-axis current reference, and the cascaded filters deteriorate the dynamics. Due to the variation of motor parameters, the q-axis current reference for the sinusoidal injection method is inappropriate, which leads to an inaccurate output torque, as illustrated in Fig. 15(b).

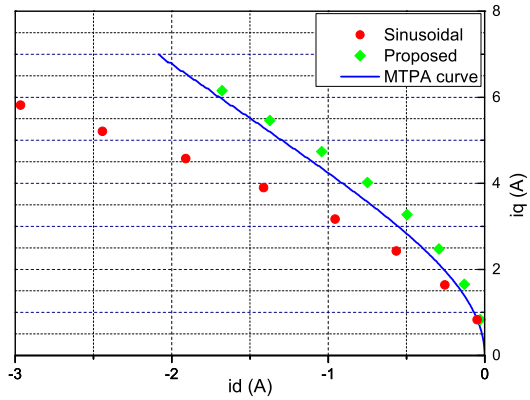

Fig. 8. The tracking accuracy of proposed method and sinusoidal signal injection method.

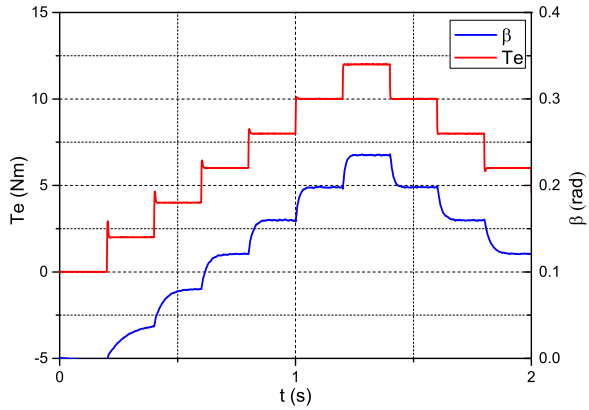

Fig. 9. Electromagnetic torque and current angle.

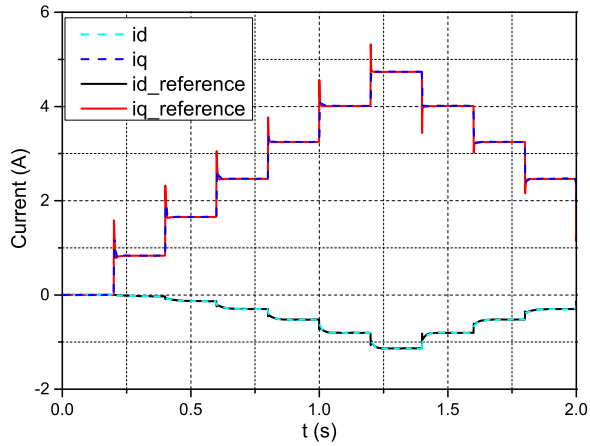

Fig. 10. d- and q-axis currents.

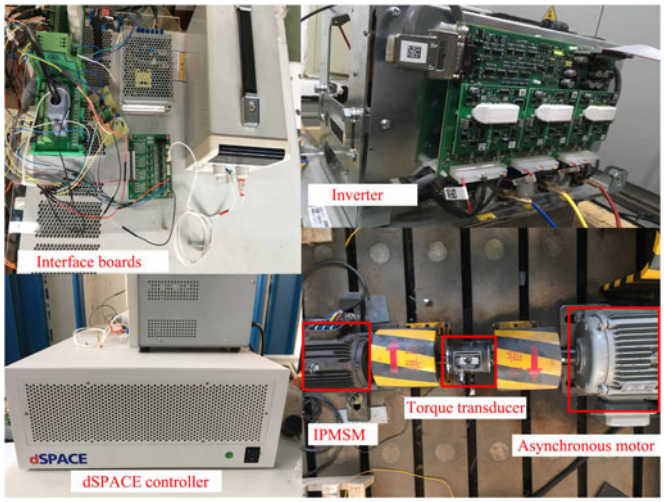

Fig. 11. Experimental setup.

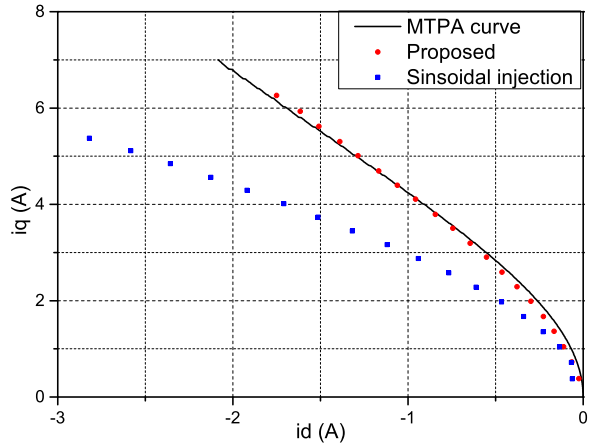

Fig. 12. MTPA tracking experimental results at the speed of 300 r/min.

The experiments of a medium speed of 600 r/min are also carried out. The torque command varies in a step of 1 N·m every 2 s, and the experimental results are illustrated in Fig. 16. It is obviously seen that the proposed method can still track the MTPA points accurately with fast dynamic response at medium speed. The proposed MTPA tracking method keeps adjusting the current angle and current vector amplitude to track the real MTPA points, and the torque responds quickly toward torque command. Obvious good accuracy can be achieved.

TABLE II
CURRENT VECTOR MAGNITUDE OF THE TWO METHODS

Torque reference	Current amplitude of the proposed method	Current amplitude of the sinusoidal signal injection method	Current amplitude difference
1 N· m	0.392 A	0.395 A	0.0031 A
5 N· m	1.72 A	1.73 A	0.01 A
10 N· m	3.34 A	3.38 A	0.04 A
15 N· m	4.98 A	5.05 A	0.07 A
20 N· m	6.63 A	6.74 A	0.11 A

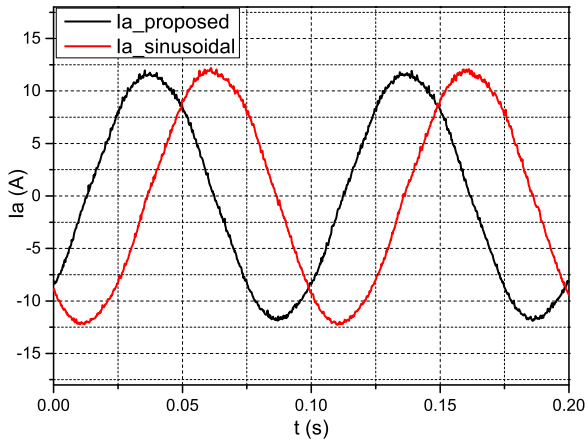

Fig. 13. Current waveform of phase A for the proposed method and the sinusoidal injection method.

To thoroughly validate the robustness of the proposed method, the experiments of the rated speed, i.e., 800 r/min with continuous step decrease torque command are carried out. The torque command decreases 1 N·m every 2 s, and the experimental results are illustrated in Fig. 17.

As the torque decreases, the initial current angle lies on the downhill side of Fig. 2, and the torque derivative is negative. Hence, the optimal current angle keeps decreasing. Good accuracy is still guaranteed under the rated speed. The proposed MTPA tracking method shows good accuracy, dynamic response, and robustness in a wide speed range under the rated speed.

To further demonstrated the dynamic process, another experiment under 800 r/min with a step change of torque reference from 0 to 10 N·m is illustrated in Fig. 18. As the torque reference increases, the current vector magnitude overshoots immediately as analyzed before, and with the current angle remains unchanged, the torque derivative becomes positive. Thus, the optimal current angle keeps increasing and the torque derivative regresses back to zero. With the help of integrals, the current vector magnitude and optimal current angle converge to the steady-state value. As the cascaded filters are removed, good dynamic response is achieved.

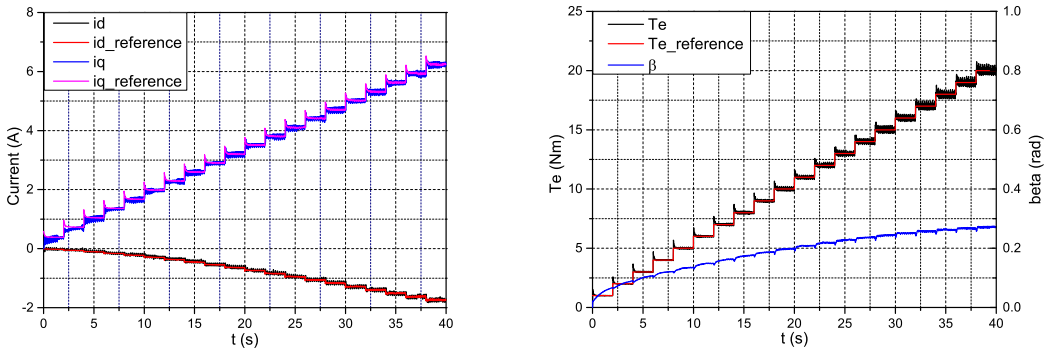

Fig. 14. Measured results of the proposed method at 300 r/min. (a) Experimental results of dq-axis currents at 300 r/min. (b) Experimental results of the output torque and the current angle at 300 r/min.

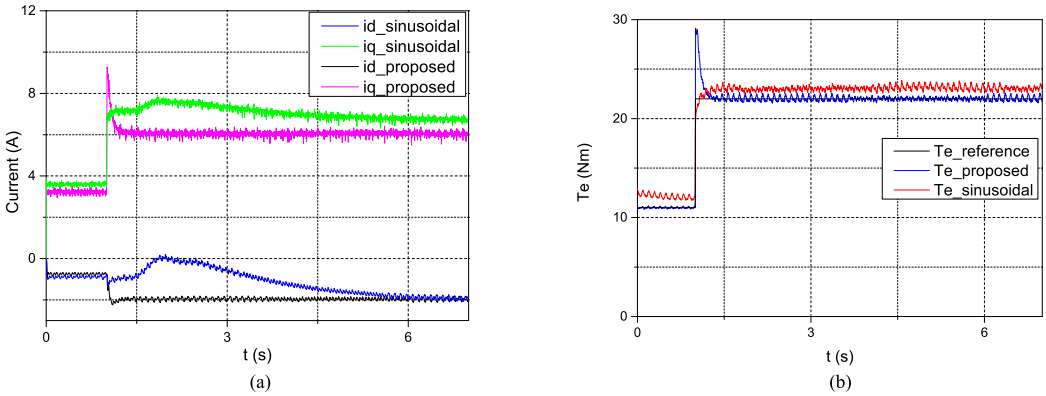

Fig. 15. Experimental comparisons between the proposed method and the sinusoidal injection method. (a) Experimental comparisons of dq-axis currents at 300 r/min. (b) Experimental comparisons of the output torque at 300 r/min.

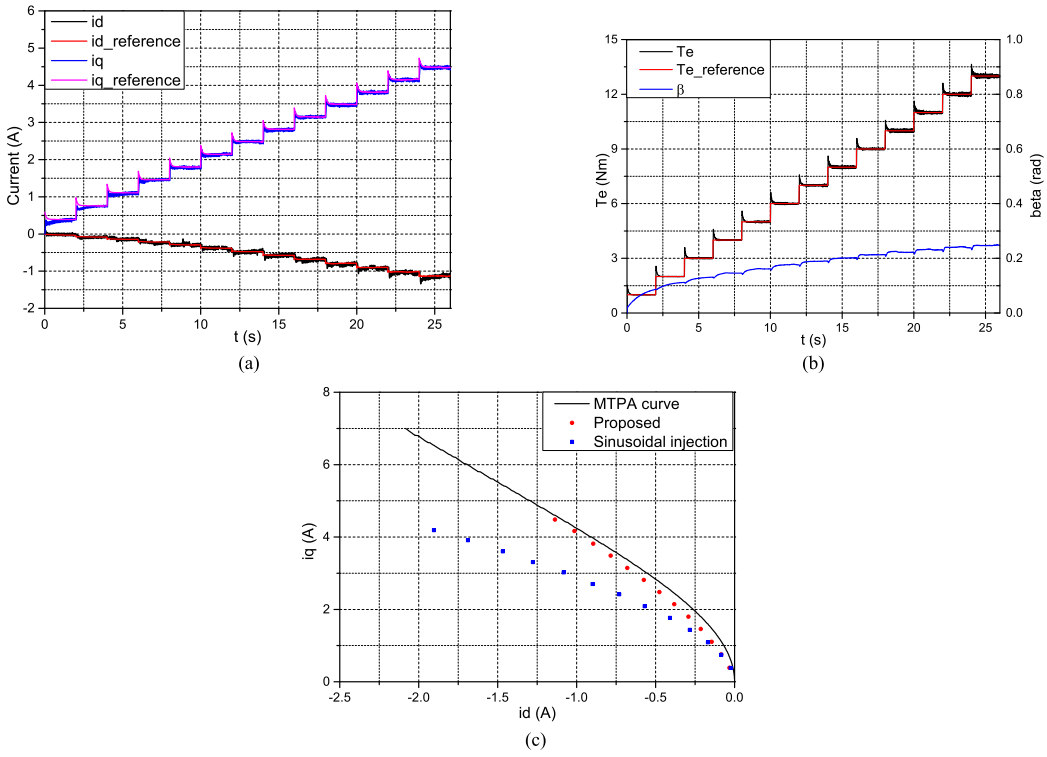

Fig. 16. Measured results of the proposed method at 600 r/min. (a) Experimental results of dq-axis currents at 600 r/min. (b) Experimental results of the output torque and the current angle at 600 r/min. (c) Experimental results of the accuracy of the proposed method at 600 r/min.

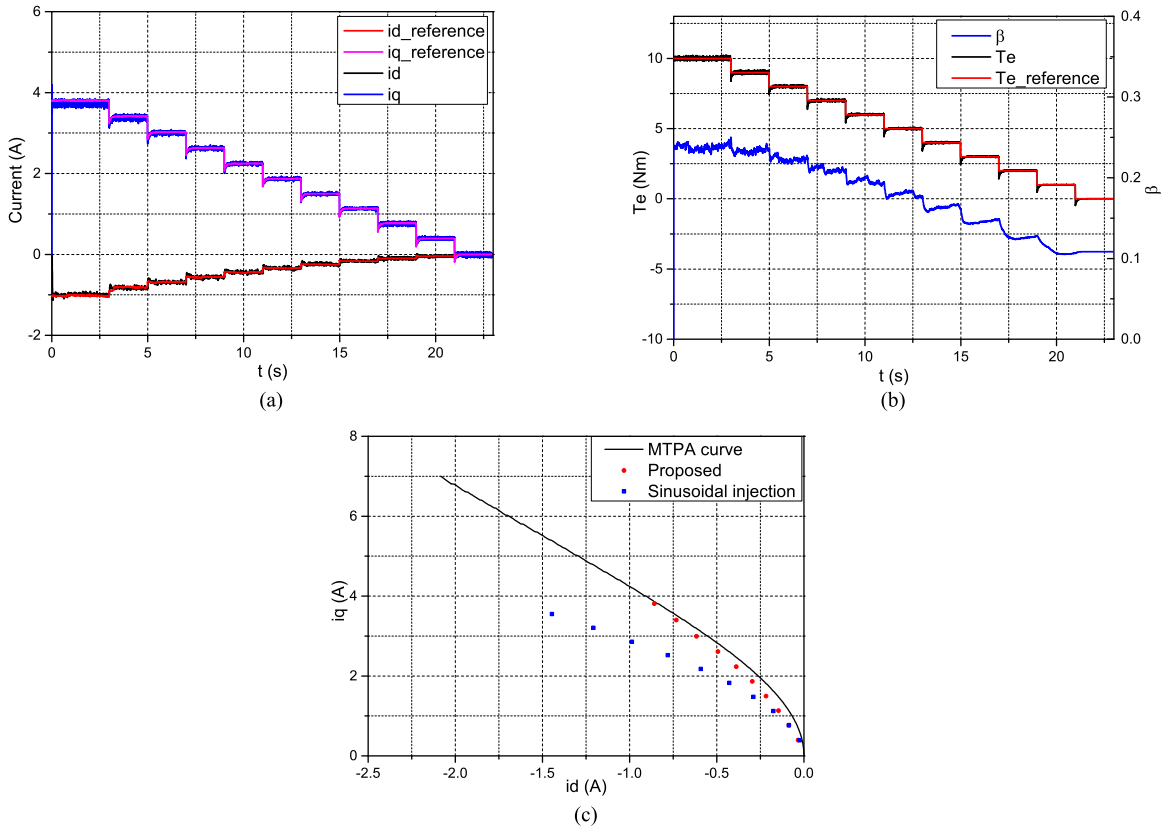

Fig. 17. Measured results of the proposed method at 800 r/min. (a) Experimental results of dq-axis currents at 800 r/min. (b) Experimental results of the output torque and the current angle at 800 r/min. (c) Experimental results of the accuracy of the proposed method at 800 r/min.

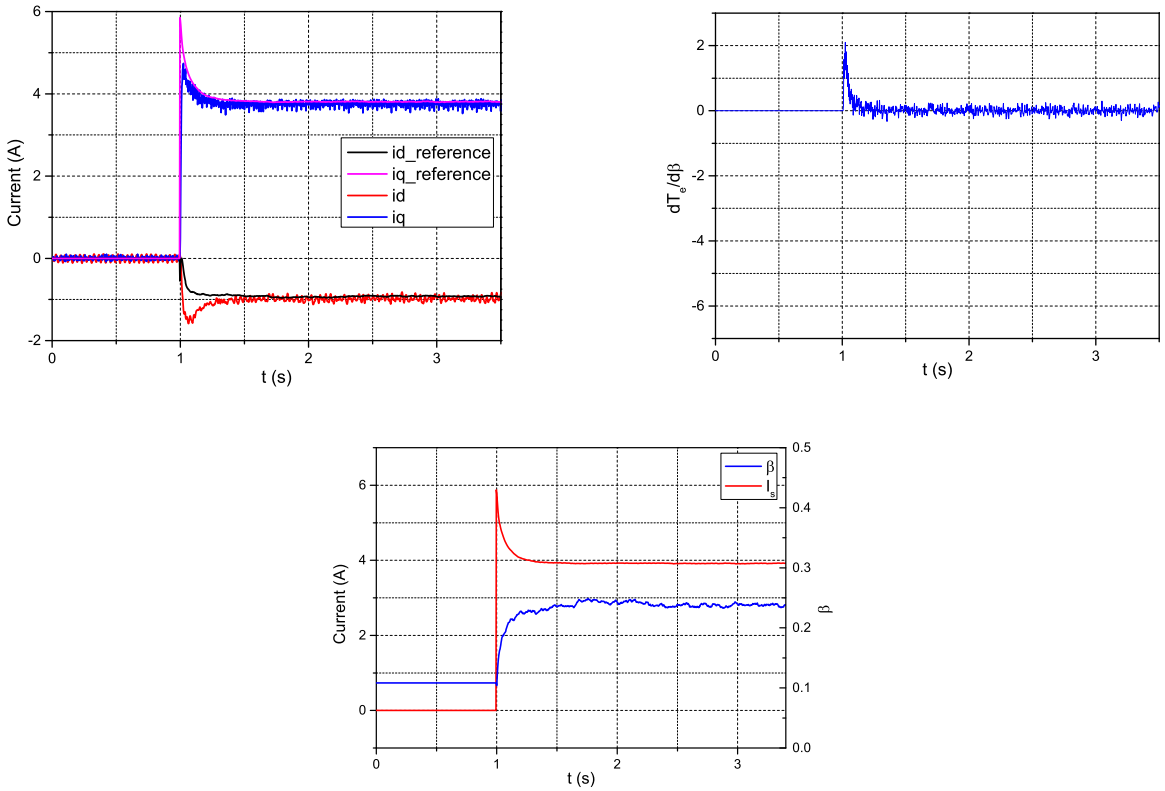

Fig. 18. Measured results of the proposed method at 800 r/min with step torque increase. (a) Experimental results of dq-axis currents at 800 r/min with step torque increase. (b) Experimental results of the torque derivative at 800 r/min with step torque increase. (c) Experimental results of the current vector magnitude and the optimal current angle at 800 r/min with step torque increase.

VI. Conclusion

This paper proposes a novel virtual square wave signal injection method to track the real MTPA points accurately with fast dynamic response utilizing the fact that torque derivative to current angle equals zero at an MTPA point. Without various filters to extract the derivative of torque to current angle, the proposed method shows fast dynamic response, and the derivative of torque to current angle is utilized to generate the current angle rather than d-axis current reference, which enhances the dynamic response as well. A more accurate equation of electromagnetic torque after signal injection guarantees the accuracy of MTPA tracking. The method to generate current vector magnitude for the torque mode is illustrated. The d- and q-axis current references are obtained through the current vector magnitude and the optimal current angle without the utilization of variable motor parameters, which guarantees the accuracy of the output torque. The high-frequency signal is mathematically injected instead of injecting into current, and thus, the problems of traditional high-frequency signal injection method such as more copper losses, current and voltage harmonics sensitivity, can be avoided. Simulations and experiments are carried out, and the results demonstrate that the proposed control scheme can accurately track the MTPA points without accurate knowledge of motor parameters and possesses fast dynamic response.

References

[1] J.-M. Kim and S.-K. Sul, "Speed control of interior permanent magnet synchronous motor drive for the flux weakening operation," *IEEE Trans. Ind. Appl.*, vol. 33, no. 1, pp. 43–48, Jan./Feb. 1997.

[2] Y.-C. Kwon, S. Kim, and S.-K. Sul, "Voltage feedback current control scheme for improved transient performance of permanent magnet synchronous machine drives," *IEEE Trans. Ind. Electron.*, vol. 59, no. 9, pp. 3373–3382, Sep. 2012.

[3] S. Morimoto, M. Sanda, and Y. Y. Takeda, "Wide-speed operation of interior permanent magnet synchronous motors with high-performance current regulator," *IEEE Trans. Ind. Appl.*, vol. 30, no. 4, pp. 920–926, Jul./Aug. 1994.

[4] S. Morimoto, K. Hatanaka, Y. Tong, Y. Takeda, and T. Hirasa, "Servo drive system and control characteristics of salient pole permanent magnet synchronous motor," *IEEE Trans. Ind. Appl.*, vol. 29, no. 2, pp. 338–343, May/Apr. 1993.

[5] K. Liu and Z. Q. Zhu, "Online estimation of the rotor flux linkage and voltage-source inverter nonlinearity in permanent magnet synchronous machine drives," *IEEE Trans. Power Electron.*, vol. 29, no. 1, pp. 418–427, Jan. 2014.

[6] S. Ichikawa, M. Tomita, S. Doki, and S. Okuma, "Sensorless control of permanent-magnet synchronous motors using online parameter identification based on system identification theory," *IEEE Trans. Ind. Electron.*, vol. 53, no. 2, pp. 363–372, Apr. 2006.

[7] S. Jung, J. Hong, and K. Nam, "Current minimizing torque control of the IPMSM using Ferrari's method," *IEEE Trans. Power Electron.*, vol. 28, no. 12, pp. 5603–5617, Dec. 2013.

[8] R. Ni, D. Xu, G. Wang, L. Ding, G. Zhang, and L. Qu, "Maximum efficiency per ampere control of permanent-magnet synchronous machines," *IEEE Trans. Ind. Electron.*, vol. 62, no. 4, pp. 2135–2143, Apr. 2015.

[9] G. Gallegos-Lopez , F. Gunwwan, and J. Walters, "Optimum torque control of permanent-magnet ac machines in the field-weakened region," *IEEE Trans. Ind. Appl.*, vol. 41, no. 4. pp. 1020–1028, Jul. 2005.

[10] B. Cheng and T. R. Tesch, "Torque feedforward control technique for permanent-magnet synchronous motors," *IEEE Trans. Ind. Electron.*, vol. 57, no. 3, pp. 969–974, Mar. 2010.

[11] S. J. Underwood and I. Husain, "Online parameter estimation and adaptive control of permanent-magnet synchronous machines," *IEEE Trans. Ind. Electron.*, vol. 57, no. 7, pp. 2435–2443, Jul. 2010.

[12] S. J. Kim *et al.*, "Torque ripple improvement for interior permanent magnet synchronous motor considering parameters with magnetic saturation," *IEEE Trans. Magn.*, vol. 45, no. 10, pp. 4720–4723, Oct. 2009.

[13] Q. Liu and K. Hameyre, "High-performance adaptive torque control for an IPMSM with real-time MTPA operation," *IEEE Trans Energy Convers.*, vol. 32, no. 2, pp. 571–581, Jun. 2017.

[14] Y. R. Mohamed and T. K. Lee, "Adaptive self-tuning MTPA vector controller for IPMSM drive system," *IEEE Trans. Ind. Electron.*, vol. 21, no. 3, pp. 636–644, Jan. 2006.

[15] M. A. Rahman, D. M. Vilathgamuwa, M. N. Uddin, and K.-J. Tseng, "Nonlinear control of interior permanent-magnet synchronous motor," *IEEE Trans. Ind. Appl.*, vol. 39, no. 2, pp. 408–416, Mar./Apr. 2003.

[16] G. Schoonhoven and M. N. Uddin, "MTPA- and FW-based robust nonlinear speed control of IPMSM drive using lyapunov stability criterion," *IEEE Trans. Ind. Appl.*, vol. 52, no. 5, pp. 4365–4374, Sep./Oct. 2016.

[17] S. Bolognani, L. Peretti, and M. Zigliotto, "Online MTPA control strategy for DTC synchronous-reluctance-motor drives," *IEEE Trans. Power Electron.*, vol. 26, no. 1, pp. 20–28, Jan. 2011.

[18] S. Bolognani, R. Petrella, A. Prearo, and L. Sgarbossa, "Automatic tracking of MTPA trajectory in IPM motor drives based on AC current injection," *IEEE Trans. Ind. Appl.*, vol. 47, no. 1, pp. 105–114, Jan. 2011.

[19] R. Antonello, M. Carrara, and M. Zigliotto, "Theory and implementation of a MTPA tracking controller for anisotropic PM motor drives," in *Proc. 38th Annu. Conf. IEEE Ind. Electron. Soc.*, 2012, pp. 2061–2066.

[20] T. Sun, J. Wang, and X. Chen, "Maximum torque per ampere (MTPA) control for interior permanent magnet synchronous machine drives based on virtual signal injection," *IEEE Trans. Power Electron.*, vol. 30, no. 9, pp. 5036–5045, Sep. 2015.

[21] T. Sun, J. Wang, M. Koc, and X. Chen, "Self-learning MTPA control of interior permanent magnet synchronous machine drives based on virtual signal injection," *IEEE Trans. Ind. Appl.*, vol. 52, no. 4, pp. 3062–3070, Jul./Aug. 2016.

[22] G. Kang, J. Lim, K. Nam, H. B. Ihm, and H. G. Kim, "A MTPA control scheme for an IPM synchronous motor considering magnet flux variation caused by temperature," in *Proc. IEEE Appl. Power Electron. Conf.*, 2004, pp. 1617–1621.

Jun Wang (S'17) received the B.E. degree in electrical engineering in 2014 from Zhejiang University, Hangzhou, China, where he is currently working toward the Ph.D. degree in electrical machines and drives.

His research interests include control and drive system design for a permanent magnet synchronous motor in the applications of electric vehicles.

Xiaoyan Huang (M'09) received the B.Eng. degree in control measurement techniques and instrumentation from Zhejiang University, Hangzhou, China, in 2003, and the Ph.D. degree in electrical machines and drives from the University of Nottingham, Nottingham, U.K., in 2008.

From 2008 to 2009, she was a Research Fellow with the University of Nottingham. She is currently a Professor with the College of Electrical Engineering, Zhejiang University, where she is working on electrical machines and drives. Her research interests include permanent magnet machines and drives for aerospace and traction applications and generator systems for urban networks.

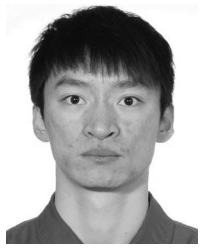

Dong Yu received the B.E. degree in electrical engineering in 2014 from Zhejiang University, Hangzhou, China, where he is currently working toward the Ph.D. degree in electrical machines and drives.

His research interests include permanent magnet machines and drives for traction applications.

Yuzheng Chen was born in Beijing, China, in 1992. He received the B.S. degree in electrical engineering in 2015 from Zhejiang University, Hangzhou, China, where he is currently working toward the M.S. degree in electrical engineering.

His main research interests include flux-weakening control of permanent magnet synchronous motors, especially for electric vehicles.

Jian Zhang received the Ph.D. degree in mechanical engineering from Zhejiang University, Hangzhou, China, in 2010.

He is currently an Assistant Researcher of electrical engineering with Zhejiang University. His current research interests include motor design and reliability analysis.

Feng Niu (M'15) was born in Hebei, China, in 1986. He received the B.S. and Ph.D. degrees from Hebei University of Technology, Tianjin, China, in 2009 and 2015, respectively, both in electrical engineering.

He is currently a Postdoctoral Fellow in the College of Electrical Engineering, Zhejiang University.

From September 2012 to September 2014, he was a Research Fellow with the Electrical Machines and Drives Laboratory, Michigan State University, East Lansing, MI, USA. He has published more than 20 technical papers in the areas of motor control and intelligent electrical equipment. His research interests include motor systems and control, power converter control, and intelligent electrical equipment.

Youtong Fang (M'11) received the B.S. and Ph.D. degrees in electrical engineering from Hebei University of Technology, Tianjin, China, in 1984 and 2001, respectively.

He is currently a Professor with the College of Electrical Engineering, Zhejiang University, Hangzhou, China. His research interests include the application, control, and design of electrical machines.

Wenping Cao (M'05–SM'11) received the B.Eng. degree in electrical engineering from Beijing Jiaotong University, Beijing, China, in 1991, and the Ph.D. degree in electrical machines and drives from the University of Nottingham, Nottingham, U.K., in 2004.

He is currently a Marie Curie Fellow with the Department of Electrical Engineering and Computer Science, Massachusetts Institute of Technology, Cambridge, MA, USA, and also a Chair Professor of Electrical Power Engineering with Aston University, Birmingham, U.K. His research interests include fault analysis and condition monitoring of electric machines and power electronics.

He Zhang (M'14) received the B.Eng. degree in control science and engineering from Zhejiang University, Hangzhou, China, in 2002, and the Ph.D. degree in electrical machines from the University of Nottingham, Nottingham, U.K., in 2009.

After receiving the Ph.D. degree, he joined the U.K. Water Research Centre, Swindon, U.K., and worked on energy efficiency determination for motor drive systems for two years. He is currently a Principal Research Fellow and Director of the Best Motion Machine Drive Technology Center within the Power Electronics, Machines, and Control Research Group, University of Nottingham Ningbo China, Ningbo, China. His research interests include high-performance electric machines and drives.